REPORT DOCUMENTATION PAGE

1. Agency Use Only *(Leave blank).*	2. Report Date. 18-21 September 1989	3. Report Type and Dates Covered. Proceedings Oceans '89

4. Title and Subtitle.
Determination of Elastic Moduli of Sea Ice

5. Funding Numbers.

Program Element No 62435N

Project No RJ035

Task No. I21

Accession No. DN496433

6. Author(s).
K.L. Williams, R. Stein, T. Wen, R.E. Francois

7. Performing Organization Name(s) and Address(es).

Applied Physics Laboratory
College of Ocean and Fishery Sciences
University of Washington
Washington, DC 98105

8. Performing Organization Report Number.

PR 89:048:242

9. Sponsoring/Monitoring Agency Name(s) and Address(es).

Naval Ocean Research and Development
Code 242
SSC, MS 39529-5004

10. Sponsoring/Monitoring Agency Report Number.

PR 89:048:242

11. Supplementary Notes.

12a. Distribution/Availability Statement.

Approved for public release; distribution is unlimited.

12b. Distribution Code.

13. Abstract *(Maximum 200 words).*

A-1

14. Subject Terms.

Acoustic Propagation; Sea Ice; Noise

15. Number of Pages. 5

16. Price Code.

17. Security Classification of Report. Unclassified	18. Security Classification of This Page. Unclassified	19. Security Classification of Abstract Unclassified	20. Limitation of Abstract

AD-A213 582

DETERMINATION OF ELASTIC MODULI OF SEA ICE

K. L. Williams, R. Stein, T. Wen, R. E. Francois

Applied Physics Laboratory
College of Ocean and Fishery Sciences
University of Washington
Seattle, Washington, 98105

ABSTRACT

For applications of elastic moduli to acoustic prediction models, moduli derived from acoustic measurements are much more appropriate than those derived from mechanical tests. Several researchers have measured sound velocity in ice and some have used these measurements to deduce ice moduli. Velocity measurement techniques include resonance vibration of ice rods, seismic and flexural wave measurement, and propagation of high frequency pulses in core samples. Differences and uncertainties in conclusions to be drawn from these studies are in part related to temperature and salinity properties of the ice and measurement and core handling procedures that have altered the structure of ice from its in-situ condition. These issues indicate the advantages of a pulse type experiment designed to allow measurement of velocities and related ice properties in the field. We present details of one such design including the equipment used and the resulting moduli uncertainties inherent in the method. The theory to be used in interpreting the experimental results will be that derived by Biot for a porous solid. Expressions for the longitudinal and shear velocities in ice were derived assuming a sealed-pore structure, which generally applies to sea ice away from the growing ice/water interface. A pilot experiment is underway at the present time to perfect the procedure and will allow preliminary implementation of the theory. The results from the type of analysis presented here ultimately lead to prediction of the acoustic impedance layers in sea ice, a crucial factor in understanding and predicting acoustic propagation processes involving sea ice.

I. INTRODUCTION

Knowledge of the vertical profiles of acoustic moduli is an important prerequisite to such tasks as ice thickness measurement or determination of the propagation into the water of sound generated on the ice surface[1]. It is also implicitly important in acoustic studies of ice keels whose raw material is undeformed sea ice. These moduli profiles can be obtained from measurements of the longitudinal and shear acoustic velocities within the ice. Three primary velocity measurement techniques have been used in both nonsaline and saline ice: seismic and flexural wave measurement,[2-4] resonance vibration of ice rods,[2,5-7] and propagation of high frequency pulses in ice cores.[7-19]

In much of the pulse technique work ice cores were taken and allowed to reach equilibrium with the air temperature or were refrigerated and taken to a laboratory for the velocity measurements. The multiphased porous nature of sea ice makes it extremely sensitive to this kind of handling procedure, which changes the *in-situ* equilibrium ratios of the liquid and solid phases as well as the properties of each phase. This in turn changes the acoustic behavior, a fact that provides sufficient motivation for design of an acoustic pulse experiment in which velocities may be obtained quickly in the field while minimizing and monitoring the change of temperature profile of the ice core and minimizing uncertainties in results. In Section II we outline the experimental equipment and procedure being developed and tested for this type of field work. We also address briefly the uncertainties in elastic moduli that result from experimental limitations. In addition to field type experiments this same type of apparatus will be useful

in conducting experiments tailored to the needs of recently obtained theoretical results for longitudinal and shear velocities using the Biot porous media theory.[20,21] The Biot theory is a natural one for porous sea ice. Experimentally, the difficulty lies in the need to specify a large number of parameters in the full Biot theory for an anisotropic open-pored medium.[22] However, if one specializes the theory to examine a closed-pore isotropic porous media (which is probably most applicable away from the ice/water interface), the number of needed parameters reduces to seven, all of which are easily interpreted physically and are amenable to experimental determination. Even with this specialization the results represent a generalization of previous models.[23] These theoretical results will be discussed in Section III, and the current status of the knowledge of each parameter will be addressed. Conclusions and summarization are given in Section IV.

II. EXPERIMENT

The primary concern in the experiment is measurement of acoustic velocities before significant temperature change occurs in the ice cores. In order to minimize the change of temperature with time, the cores are wrapped in closed-cell foam immediately after withdrawal. After wrapping, 1/8th inch diameter holes are drilled into the core at regular intervals and temperatures recorded with a digital thermometer accurate to $0.2°$ C. The cores are then sectioned in a mitre box (in 5-10 cm lengths), each section being centered around the temperature monitoring holes. Starting with the section furthest from ambient temperature, the time of flight and section length are measured using the apparatus shown in Fig. 1. Identification and description of the equipment is made in the figure caption. The sending transducer at one end of the sample holder is excited by a pulser/receiver, and the delayed signal acquired by the receiving transducer is amplified by the same pulser/receiver and output on a 10 MHz digital scope where it is stored on the built-in disc memory. The caliper attached to the sample holder has a resolution of 0.001 inches; however, roughness of the section ends and use of a coupling gel lead us to use a more conservative estimate of length uncertainty, i.e., measurements to 0.01 inches are realizable in practice. The scope is triggered by a sync pulse sent out at the time of sender excitation so that the time of flight is directly measurable. Inherent delay and "zero" sample length are checked beforehand with sender and receiver in direct contact. Also, time of flight measurements on calibrated aluminum and granite rods allow elimination of systematic time scale errors.

After the time of flight measurement, the temperature of the core section is again measured, the sample density is determined, and the sample is placed in a sealable container and allowed to melt. After melting, a salinity measurement with an accuracy better than 0.1 ppt is made using a conductivity cell.[24] Previous APL in-field experimental measurements of core section density have shown that hydrostatic measurements of densities accurate to 0.001 gm/cm^3 are achievable. However, the present method is time consuming and there is some small unavoidable temperature cycling. The technique and uncertainties involved are discussed in Ref. 25. The main concern is determination of whether air is entrapped within the section. Changes in density due to air content are known to be small (on the order of 0.03 gm/cm^3); however,

introduction of air introduces another degree of freedom that may have a large, frequency dependent effect on acoustic velocities (see the end of Section III).

The object of the experiment is to determine ice acoustic moduli and their dependence on the temperature and salinity of the ice. Before discussing the uncertainties of the resulting moduli values, it is important to decide which moduli are most appropriate to determine. Previous analyses have concentrated on determining Young's modulus and Poisson's ratio.[26] However, for comparison with Biot porous solid results, it is more natural (see Section III) to determine the effective bulk modulus K^{eff}_i and shear modulus μ^{eff}_i of the ice (which moduli to concentrate on is, of course, simply a matter of convenience since the various moduli are interrelated). These moduli may be determined from velocity and density (ρ_i) measurements via the equations

$$c_1 = \sqrt{(K^{eff}_i + \frac{4\mu^{eff}_i}{3})/\rho_i} \qquad (1)$$

$$c_s = \sqrt{\frac{\mu^{eff}_i}{\rho_i}} \qquad . \qquad (2)$$

In Section III these effective moduli will be given in terms of the moduli found in the Biot model results for a sealed-pore porous solid. Using Eqs. 1 and 2 , the measurement uncertainties given in the previous paragraphs as the limiting errors, and assuming an 8 cm core section length with $c_1 \approx 4000$ m/s and $c_s \approx 2000$ m/s, the lowest uncertainties $\delta\mu^{eff}_i$, δK^{eff}_i obtainable from individual measurements are approximately

$$\delta\mu^{eff}_i \approx 1.3\% \ \mu^{eff}_i \qquad (3a)$$

$$\delta K^{eff}_i \approx 3.6\% \ K^{eff}_i \qquad . \qquad (3b)$$

These moduli values are to be associated with temperature (T) and salinity (S) values whose uncertainties are also given in the above paragraphs so that one may find $K^{eff}_i(T,S)$ and $\mu^{eff}_i(T,S)$. Our pilot experiments are aimed at perfecting experimental procedure so as to approach these instrumentation limits.

Before proceeding to theoretical results, it is appropriate to examine briefly the type of uncertainties in moduli we expect due to the uncertainties in measurements of T and S. This calculation requires knowledge of the functional dependence of the moduli on T and S, which is actually the relation being sought so this uncertainty determination may seem somewhat premature (or impossible). However, we can obtain an estimate for the uncertainty of the bulk modulus by using previous results for the functional dependence of the Young's modulus of sea ice on porosity[26] (β), the empirical result that the Poisson's ratio of ice is close to 1/3 (Refs. 7, 26), as well as the Frankenstein-Garner equation relating β to T and S. If the Poisson's ratio of sea ice is assumed equal to 1/3, then the effective bulk modulus is equal to the Young's modulus.[26] Using Fig. 19 of Ref. 26 to determine a linear approximation for the relation between porosity and modulus, then relating porosity to S and T using Eq. 13 of Ref. 27, one can derive the relations

$$K^{eff}_i \approx 1.0 \times 10^{11} - (2.0 \times 10^{11}) \beta \qquad (4a)$$

$$K^{eff}_i \approx 1.0 \times 10^{11} - (2.0 \times 10^9) S (0.0532 - \frac{4.919}{T}) \qquad . \qquad (4b)$$

In this relation β is the volume of brine divided by total volume of an ice sample, S is in ppt, the Frankenstein-Garner equation used is appropriate for $-0.5^\circ C < T < -23^\circ C$, and the resulting modulus is in units of dynes per cm^2. The approximation in Eq. 4a is limited to values of $\beta \le 0.5$ since the bulk modulus must be positive. The Biot model of the next section shows that the β range of this approximation must be further restricted to $0 \le \beta \le 0.25$ if physical values of Biot moduli are to result from its use. Using Eq. 4b, the uncertainty in K^{eff}_i is a function of the values T and S. Uncertainties for a few combinations of T and S are shown in Table I.

T (C)	S (ppt)	β (%)	δT (C)	δS (ppt)	δK/K (%)
-2.0	4.0	10	0.2	0.1	3.1
-2.0	10.0	25	0.2	0.1	10.8
-2.0	10.0	25	0.2	0.05	10.4
-5.0	4.0	4	0.2	0.1	0.5
-5.0	10.0	10	0.2	0.1	1.3
-5.0	10.0	10	0.2	0.05	1.1
-20.0	4.0	1	0.2	0.1	0.1
-20.0	10.0	4	0.2	0.1	0.1
-20.0	10.0	4	0.2	0.05	0.08

Table I. Uncertainties in the effective bulk modulus resulting from uncertainty in measured values of T and S are shown for various combinations of T, S, δS, and δT.

If the time of flight determination of the bulk modulus were without uncertainty, an individual modulus value could be associated with a (T,S) set of experimental values only to within the uncertainties given in the last column. Thus time of flight derived modulus uncertainties (Eq. 3) less than what is shown in the last column are not productive until equipment-limited uncertainties in T and S are lowered. The uncertainty in K^{eff}_i is largest for temperatures near freezing and high salinities. Physically, this is because the porosity is quite large (≈ 25 %) and very sensitive to temperature changes. Four comments are appropriate: Eq. 4 from which the table is derived is untested experimentally at porosities above about 10%; experimental difficulties due to brine drainage probably represent a much bigger challenge at temperatures near freezing than temperature uncertainty; the acoustic velocity determined from a bulk modulus known to within 10% will only be in error by about 5%; at colder temperatures time of flight errors are the major contributors to bulk modulus uncertainty.

III. BIOT THEORY

The porous nature of saline ice[27] is responsible for its differences in behavior relative to fresh water ice. This porous nature has been taken into account in varying degrees in some analyses. In particular Refs. 15 and 23 discuss calculations of sound velocities in which the saline ice is modeled as a matrix of solid ice with the inherent Young's modulus of ice and pores filled with brine. A consequence of this type of model is that the Young's modulus depends only on the intrinsic Young's modulus of ice, the bulk modulus of the brine, and the porosity (Eq. 9.34 of Ref. 23). However, experimental results in Ref. 7 for Young's modulus of summer and winter ice with the same porosity indicated differing behavior for the same porosity. This was tentatively identified as due to differences in the solid matrix (thus implying use of the intrinsic Young's modulus of fresh water ice for the matrix might be an incomplete representation).

The above discussion indicates the desirability of a model that allows explicitly for the variation in the ice matrix as conditions (i.e., T and S) change. The Biot model[20,21] of a porous solid is one means of including ice matrix variations. However, use of the full Biot theory for an open-pored anisotropic material requires the

determination of 17 parameters.[22] At least initially, it is useful to specialize the most general Biot results to reduce the number of parameters while still retaining enough complexity that the results represent a generalization of previous analyses.

Reiterating from Section I, the specialization that we use consists of assuming the brine-filled pores in the saline ice are sealed and that the ice is isotropic. The sealed-pore assumption is most valid away from the skeletal layer at the water/ice interface.[27] With this restriction the number of parameters that must be specified is reduced to seven, which are easily interpreted. Before synopsizing the results derived using Biot theory, it is appropriate to point out that since the model, as derived by Biot, was for a two-phase problem (i.e., liquid/solid, gas/solid, etc.) it may not reliably predict behavior in a three-phase situation (liquid/gas/solid). Further comment about the three phase situation will be made at the end of this section.

The terminology to be used here mirrors that of Ref. 28. A complete development of Biot's theory may be found in Refs 20, 21, 29, and 30. We simply note here that Biot's examination of propagation of energy through a porous material began with a determination of the potential energy stored within the material and the kinetic energy due to the motion of both the solid and liquid phases. With these he could write the Lagrangian density and determine the equations of motion. From this type of analysis one can derive a set of coupled equations of motion for the liquid and solid. These equations are given as Eq. 6 of Ref. 28 (we note a typographical error in the first of those equations, i.e., 2μ should be replaced by μ). These equations are coupled via the relative motion of the liquid and solid. Assuming a sealed-pore structure eliminates this relative motion. To correctly handle this situation within the context of Biot theory, one must go back to the potential and kinetic energy equations[29,30] and eliminate the relative motion. In doing so one finds that only one equation survives and is of the form

$$\mu_b \nabla^2 \vec{u} + (H-\mu_b)\nabla(\nabla \cdot \vec{u}) = \rho \frac{\partial^2 \vec{u}}{\partial^2 t} \quad , \tag{5}$$

where

$$\rho = \beta\rho_f + (1-\beta)\rho_s \quad .$$

In these equations $\vec{u}$ is a displacement vector for differential volume of the solid, μ_b is the shear modulus of the frame, ρ is the total mass density, ρ_f is the fluid density, ρ_s is the solid density, and H is the combination of bulk moduli for the frame, solid, and fluid given below. If the displacement vector is written as a combination of scalar (ϕ) and vector (ψ) potentials

$$\vec{u} = \nabla\phi + \nabla\times\psi \quad , \tag{6}$$

then Eq. 6 can be rewritten as two equations

$$H\nabla^2\phi = \rho\ddot{\phi} \tag{7a}$$

$$\mu_b\nabla^2\psi = \rho\ddot{\psi} \tag{7b}$$

where the double dots represent partial differentiation with respect to time. Assuming monochromatic solutions for the potentials[31] one can arrive at the following longitudinal and shear wave velocities

$$c_l = \sqrt{\frac{H}{\rho}} \tag{8a}$$

$$c_s = \sqrt{\frac{\mu_b}{\rho}} \quad . \tag{8b}$$

Substitution of the expression for H (Ref. 30) gives our desired results

$$c_l = \sqrt{\frac{[(K_r-K_b)^2/(K_r(1 + \beta(K_r/K_f - 1))-K_b)] + K_b + 4\mu_b/3}{\beta\rho_f + (1 - \beta)\rho_s}} \tag{9}$$

$$c_s = \sqrt{\frac{\mu_b}{\beta\rho_f + (1 - \beta)\rho_s}} \quad . \tag{10}$$

In this expression, in addition to previously defined quantities, K_r is the bulk modulus of nonsaline ice, K_f is the bulk modulus of the pore brine, and K_b is the bulk modulus of the ice frame. These expressions are novel in that they allow one to explicitly see the dependence of the acoustic velocities on porosity and frame rigidity. Comparison of Eqs. 9 and 10 with Eqs 1 and 2 shows that

$$\mu^{eff}_i = \mu_b \tag{11}$$

$$K^{eff}_i = \left[\frac{(K_r-K_b)^2}{(K_r(1 + \beta(K_r/K_f - 1))-K_b)}\right] + K_b \tag{12}$$

$$\rho_i = \beta\rho_f + (1 - \beta)\rho_s \quad . \tag{13}$$

The results in Eqs. 9-13 represent a generalization of results based on simpler theories. In particular, to recapture velocity results from suspension theory[32] one sets K_b and μ_b equal to zero. To obtain the Young's modulus in Eq. 9.34 of Ref. 23 (see beginning of this section), one assumes Poisson's ratio is zero[23] and sets $K_b = (1-\beta)K_r$. Setting $K_b = (1-\beta)K_r$ is equivalent to assuming the ice within the frame matrix has a bulk modulus equal to the inherent modulus of ice. Clay and Medwin[33] have derived an expression equivalent to Eq. 12 via a different method.

The results above indicate that seven parameters are needed to characterize a closed-pore, air-free Biot solid, i.e., β, ρ_s, ρ_f, μ_b, K_b, K_s, K_f. All are easily interpreted physically. Of the seven parameters, two depend on temperature (K_s, ρ_s) and the rest on both salinity and temperature. It is anticipated that characterization of the ice cores examined via the experimental procedure of Section II will be completed as follows. The values of S and T will be used to determine β, ρ_f, and ρ_s(T only) using Ref. 34. The consistency of these predictions with the experimentally determined ice density will be checked using Eq. 13. Low experimental values for ice density imply air content, and sections containing air (most likely in the upper few centimeters of the core) will not be analyzed in terms of the present theory (further comment on the modeling of a liquid/air/solid porous medium is made at the end of this section). For air-free sections the experimentally determined effective moduli will be used to determine μ_b, and K_b. Obtaining μ_b is trivial (cf. Eq. 11), but determination of K_b requires some explanation. First, Eq. 12 can be solved for K_b to give

$$K_b = K_s\left[\frac{\beta K^{eff}_i(K_s-K_f) - K_f(K_s-K^{eff}_i)}{\beta K_s(K_s-K_f) - K_f(K_s-K^{eff}_i)}\right] \quad . \tag{14}$$

Equation 14 shows that in addition to the experimentally determined value of $K^{eff}_i(S,T)$, we need $K_s(T)$, and $K_f(S,T)$ to obtain $K_b(S,T)$. Measurements of the temperature dependence of K_s may be found in Refs. 5 and 8. No measurements of the salinity and temperature dependence of K_f for salt water brine have been found, and at present we will assume $K_f \approx 2.0 \times 10^{10}$ dynes/cm^2. This value corresponds to an acoustic velocity in water of about 1440 m/s. Measurement of both $K_s(T)$ and $K_f(S,T)$ are needed and are amenable to well controlled laboratory experiments, implying experimental errors much lower than those inherent in the current measurement of effective moduli. A preliminary estimate of the error in the values of K_b due to the errors in K^{eff}_i can be established using Eq. 14, the approximation of Eq. 4a, and using the fact that K_f is found to equal approximately 0.2 K_s. With these assumptions $K_b \approx (1-4\beta) K_s$ and the partial derivative of K_b with respect to K^{eff}_i is found to equal approximately 4, implying an error in measurement of $K_b(S,T)$ of 0.14 $K^{eff}_i(S,T)$ for the error in Eq. 3. The result for K_b implies that the relation in Eq. 4a cannot be used for $\beta \geq 0.25$ since physically $0 \leq K_b \leq K_s$. It is important to emphasize that one of the major uses of the Biot moduli will be to predict acoustic velocities in ice, and if the error in K_b is traced backward, it implies velocity results to less than 2% error.

A comment on inclusion of air in the porous solid model is in order to conclude this section. Bedford and Stern[35] have extended the Biot model to include content of a small volume of air bubbles. Their results indicate that above the resonance frequencies of the air bubbles, the velocity of the longitudinal wave examined here would be essentially the same. However, below the bubble resonance frequency, the velocity would be substantially depressed and at resonance the velocity goes through a maximum. The applicability of their analysis in obtaining ice acoustic velocities is currently being examined.

IV. SUMMARY AND CONCLUSIONS

An experiment currently being tested for in-field measurement of ice moduli has been outlined. The in-field nature of the experiment is a requirement of the sensitivity of saline ice to handling procedures. The moduli to be extracted are those needed in the Biot model specialized to an isotropic, sealed-pore, air-free porous solid. The specialization reduces the number of parameters needed to seven while still generalizing previous results. Operationally, the end product of these kind of experiments is an increase in the accuracy of measuring and predicting velocity profiles from relatively simple measurements of the physical parameters (S,T), and therefore an increase in the accuracy of analyses and tasks that use them.

The Biot model has been experiencing increased use in recent years. Its major drawback is the need to experimentally measure many parameters. Since the model is only as good as the parameter measurements, it is important that experimental parameter measurement efforts be initiated. The work here is in part motivated by the need for accurate parameter determination. Experience with the present model, in which the number of parameters are restricted and easy to interpret physically, is an important first step to measurements of parameters in more general situations.

ACKNOWLEDGMENTS

REFERENCES

1. T. Wen, and R. Francois, IEEE Oceans'89 Conference Proceedings, Sept.18-21, 1989.

2. J. H. Brown, and E. E. Howick, NEL Research and Development Report 825 (U. S. Navy Electronics Laboratory, San Diego, Cal.) (1958).

3. J. H. Brown, in Ice and Snow: Properties, Processes, and Applications, Cambridge, Mass.: MIT Press, pp. 79-106 (1963).

4. D. L. Anderson. Trans. Eng. Inst. Canada, Vol. 2, No. 3, pp. 116-122 (1958).

5. R. W. Boyle, and D. O. Sproule, Can. J. Research, Vol. 5, pp. 601-618 (1931).

6. T. D. Northwood, Can. J. Research, Vol. 25, part A, pp. 88-95 1947)

7. M. P. Langleben, and E. R. Pounder, in Ice and Snow: Properties, Processes, and Applications, Cambridge, Mass.: MIT Press, pp. 69-78 (1963).

8. V. V. Bogorodskii, Sov. Phys. Acoust., Vol. 4, pp. 17-21 (1958).

9. E. R. Pounder, and P. Stalinsky, Int. Assoc. of Scientific Hydro., Publ. 54, pp. 35-39 (1960).

10. M. P. Langleben, Can. J. Phys., Vol. 40, No. 1, pp. 1-8 (1962).

11. V. V. Bogorodskii, Sov. Phys. Acoust., Vol. 10 No. 2, pp. 124-126 (1964).

12. G. Abele, and G. Frankenstein, CRREL Report - 176 (1967).

13. H. F. Bennett, CRREL Research Report - 237 (June 1972).

14. R. E. Bunney, Appl. Phys. Lab - Univ. Wash. Report 7317, (April 1974).

15. V. V. Bogorodskii, V. P. Gavrilo, A. V. Gusev, and V. A. Nikitin, Sov. Phys. Acoust., Vol. 21, No. 3, pp. 286-287 (1975).

16. V. V. Bogorodskii, V. P. Gavrilo, and V. A. Nikitin, Sov. Phys. Acoust., Vol. 22, No. 2, pp. 158-159 (1976).

17. H. Kohnen, and A. J. Gow, J. Geophys. Research, Vol. 84, No. C8, pp. 4865-4873 (1979).

18. C. H. Yew, in Proceedings of the Arctic Oceanography Conference and Workshop, Naval Ocean Research and Development Activity, NSTL, Mississippi (1985).

19. P. J. Vidmar, Applied Research Lab. - Univ. Texas Report 87-6, (Feb. 1987).

20. M. A. Biot, J. Acoust. Soc. Am., Vol. 28, pp. 168-178 (1956).

21. M. A. Biot, J. Acoust. Soc. Am., Vol. 28, pp. 179-191 (1956).

22. C. H. Yew, and X. Weng, J. Acoust. Soc. Am., Vol. 82, pp. 342-353 (1987)

23. Bergdahl, Report series A:1, Dept. of Hydraulics, Chalmers Univ. of Tech. (1977).

24. G. R. Garrison, T. Wen, R. E. Francois, and W. J. Felton, and W. L. Welch, Applied Physics Lab - University of Washington Report 4-86 (1987)

25. P. Becker, APL internal report (1986).

26. M. Mellor, CRREL Report 83-1 (1983).

27. G. A. Maykut, Applied Physics Lab Report 8510 (1985)

28. R. Stoll, and T. Kan, J. Acoust. Soc. Am., Vol. 70, pp. 149-156 (1981)

29. M. A. Biot, J. Appl. Phys., Vol. 33, pp. 1482-1498 (1962)

30. R. D. Stoll, in Physics of Sound in Marine Sediments, Ed. by L. Hampton (Plenum, New York, 1980)

31. A. L. Fetter and J. D. Walecka, Theoretical Mechanics of Particles and Continua, Chapter 13 (McGraw-Hill, New York, 1980)

32. J. M. Hovem, J. Acoust. Soc. Am., Vol. 67, pp. 1559-1563 (1980)

33. C. S. Clay, and H. Medwin, Acoustical Oceanography: Principles and Applications, Appendix A8 (John Wiley & Sons, 1977)

34. G.F.N. Cox, and W. F. Weeks, CRREL report 82-30 (1982)

35. A. Bedford, and M. Stern, J. Acoust. Soc. Am., Vol. 72, pp. 409-417 (1983).
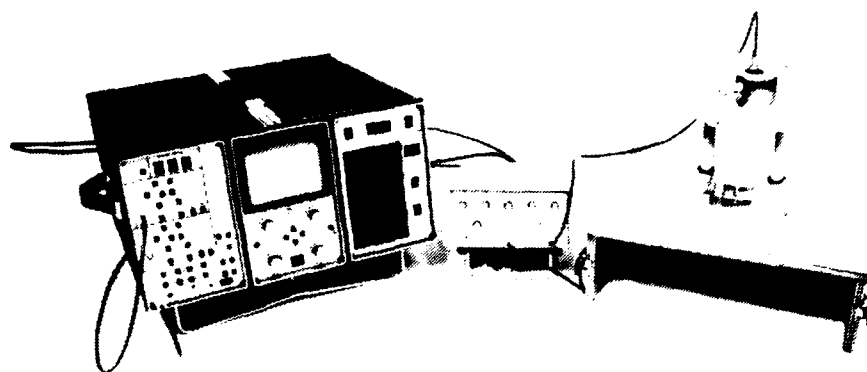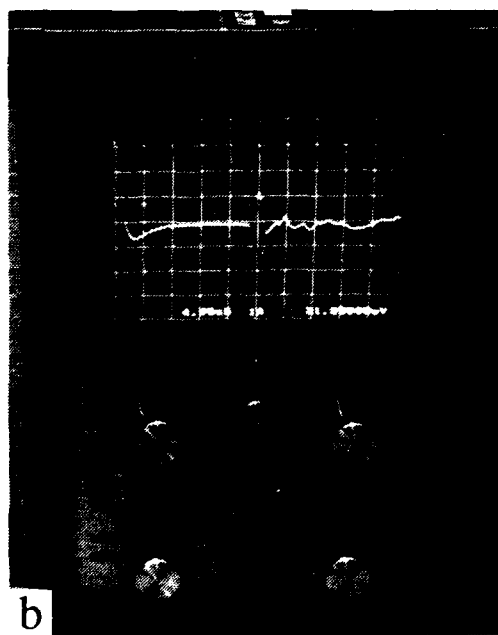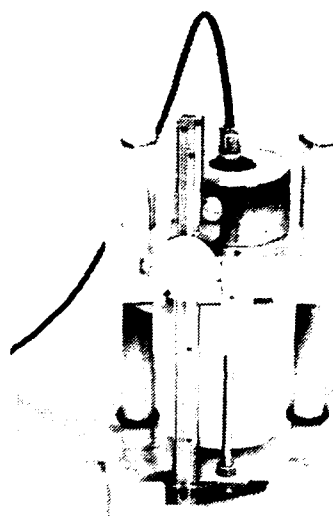
Figure 1. The in-field ice velocity measuring apparatus: a) left to right - Nicolet 4094 digitizing scope with a 10 MHz plug-in unit and built-in disc memory, Panametrics 5055PR pulser/receiver (p/r), APL built ice sample holder that houses sending and receiving transducers;b) typical received waveform after amplification by p/r unit;c) close-up of sample holder. In operation the p/r excites a broad bandwidth transducer (longitudinal or shear) coupled to the ice sample. The receiver signal is amplified by the p/r and the resulting signal displayed on the scope. Sample length is directly measurable by the caliper attached to the sample holder and time of flight is directly measurable on the scope. The emphasis is on fast/accurate data acquisition so that the physical parameters of the sample are near their in-situ values.